Author's Response to Editor's Comments on *"Brief Communication: Evaluation and comparisons of permafrost map over Qinghai-Tibet Plateau based on inventory of in-situ evidence"*

Bin Cao[1,2], Tingjun Zhang[1], Qingbai Wu[3], Yu Sheng[3], Lin Zhao[4,5], and Defu Zou[5]

[1]Key Laboratory of Western China's Environmental Systems (Ministry of Education), College of Earth and Environmental Sciences, Lanzhou University, Lanzhou 730000, China
[2]Department of Geography & Environmental Studies, Carleton University, Ottawa K1S 5B6, Canada
[3]State Key Laboratory of Frozen Soil Engineering, Cold and Arid Regions Environmental and Engineering Research Institute, Chinese Academy of Sciences, Lanzhou 730000, China
[4]School of Geographical Sciences, Nanjing University of Information Science and Technology, Nanjing 210044, Chin
[5]Cryosphere Research Station on the Qinghai-Tibet Plateau, State Key Laboratory of Cryospheric Science, Cold and Arid Regions Environmental and Engineering Research Institute, Chinese Academy of Sciences, Lanzhou 730000, China

Correspondence: Tingjun Zhang(tjzhang@lzu.edu.cn)

Response to Editor

Dear Peter Morse,

Thank you for the constructive feedback, and the detailed assessment of the manuscript. Below we provide a point-to-point response to each comment, comments are given in black, responses are given in blue.

Bests,
Bin Cao

Major:

Thank you for your revisions. You have incorporated may of the reviewers' suggestions and the document has improved as a result. However, there are still two main issues that have to be resolved.

- First, this manuscript cannot be published as is, in part, because the language is poor. From the title to the last table cation there are numerous language-use problems that need to be addressed. Both of the reviewers noted this, and R1 suggested that you work with a native speaker to improve the writing. I agree. Please work with somebody who will help correct the mistakes and improve the clarity of the text. I have included several examples of how to simplify and clarify the text, but leave it to you to complete this task for the rest of the paper.
  Response: Thanks for the examples. The manuscript was carefully revised by native speaker, and all the changes are highlighted in the revised manuscript.

- Second, as written, the study is not repeatable. The analysis hinges on the methods used to simplify categorical data in to binary data (P4, Line 19), but these methods are not described. consequently, this also makes the results difficult to interpret and rely on.
  Response: We added a paragraph in Section 2.4 Statistics and evaluation of permafrost distribution maps (see below)

  To conduct the map evaluations against measurements with binary information (presence or absence), it was necessary to develop classification aggregations for the existing maps. We argue that although the aggregation presented here simplifies the information available in these maps and may introduce uncertainty for further analyses, it is necessary in order to conduct inter-comparisons among them. For the IPA map, we consider the continuous and discontinuous permafrost zones to correspond to permafrost presence and the other zones

(sporadic permafrost, island permafrost, and non-permafrost) to correspond to permafrost absence by using the proportion of ground underlain by permafrost of 50% as a threshold. This is consistent with the threshold of the PZI map described below. For the QTP_{TTOP} and QTP_{Noah} maps, the permafrost distribution was derived using simulated mean annual ground temperature (thermally defined). In these maps, areas are classified into three type: permafrost, seasonally frozen ground, and unfrozen ground. Here, we merge the areas of seasonally frozen ground and unfrozen ground to yield areas of permafrost absence. For the PZI maps, specified thresholds are required for both the extent of permafrost region and permafrost area. Following Gruber (2012), only the areas with PZI $\geq$ 0.01 were selected for further analysis, permafrost regions were defined as where PZI $\geq$ 0.1, and permafrost area was calculated as PZI multiplied pixel area. A value of 0.5 was used as the threshold of permafrost presence and absence (Boeckli et al. , 2012; Azócar et al. , 2017).

There is a big mistake in the previous version. All the four permafrost types (continous, discontinous, sporadic, and island) in the IPA map were aggregated to permafrost presnece. This resulted in significant overestimatiton of permafrost distribution. Now we corrected the aggregation as described above.

Once you have revised the manuscript, I will accept Reviewer 1's offer, and ask for a second review. I think that by then the manuscript will be ready for publication.

Thank you for your work, and I look forward to a revised version.

Best regards,

Peter

Specific:

Response: Thank you for the detailed editing. The language was corrected as suggested throughout the manuscirpt if not specified, and changes are highlighted in the marked-up manuscript version. We only listed the logic and technique comments below.

- P1, 12: Change "Cheng and Jin (2013)" to "Cheng and Jin, 2013", "Mu et al. (2017)" to "Mu et al., 2017", and "Wu et al. (2016)" to "Wu et al., 2016"
  Response: Corrected throughout the manuscript.

- P2, L2: In addition to what? The logic of this sentence do not follow from the previous.
  Response: The sentence was change to *"The QTP has also been included in ...."* to clarify.

- P2, L8: Gap in logic. Make it clear to the reader: How does having an improved evaluation improve the application of the existing maps?
  Response: This part was changed to

  "A new inventory of this field evidence provides an opportunity to improve the evaluation of the existing permafrost maps. This is an important step in describing the current body of knowledge on permafrost mapping performance as well as identifying any possible bias. It is also critical for identifying priorities when updating these maps in the future. Additionally, an improved evaluation is a useful guide to selecting a map to use for permafrost and related studies, for example as a boundary condition for eco-hydrological model simulations."

  to clarify.

- P2, L18: I think that Table A1 should be included within the main document. If the writing is improved in this section, it and the information on page 7, lines 20-24, can be incorporated quite well.
  Response: We agree. The table as well as the appendix A1 "Classification algorithm of in-situ permafrost presence or absence evidence" were merged into the main text (Section 2.1 Inventory of permafrost presence/absence evidence).

  "In order to apply the permafrost presence or absence inventory more broadly, the degree of confidence in the data is estimated and provided in the inventory and in Table **??***, although it is not used in this study. BH and SP provide direct evidence of permafrost presence or absence based on MGT and/or ground ice observations, and hence have high confidence (Cremonese et al., 2011). The data confidence derived from MAGST is classified*

based on temperature and the length of the observation period. The evaluated GPR survey result was considered to have medium confidence."

- P2, L19: MAGT is often used when referring to the temperature at the depth of zero annual amplitude. Do you simply mean mean ground temperatures?

- P2, L19: The way this sentence is written, it seems like temperature varies in length.
Response: This is the response for above two specific comments. We changed the MAGT to "mean ground temperature (MAT)" throughout the manuscript to clarify. Yes, the borehole temperature used here veried depending on the depth of zero annual amplitude and measured depth. The sentence is changed to

"In this study, we used the mean ground temperature (MGT) measured from the borehole, the depth of which varies from meters to about 20 m depending on the depth of zero annual amplitude and borehole depth, to identify permafrost presence or absence."

- P2, L21: Change "1 meter" to "1 m"
Response: Corrected.

- P2, L21: This sentence doesn't make sense. Please clarify.
Response: It is deleted.

- P2, L23: Define the thermal offset for readers. Lin et al., 2015, Permafrost and Periglacial Processes, discuss a reversed thermal offset in QTP. You may want to include something from it here.
Response: Thermal offset is defined as *"the mean annual temperature at the top of permafrost minus MAGST"*, and reversed thermal offset is discussed. This GST part is changed to

"Thermal offset is defined as the mean annual temperature at the top of permafrost (TTOP) minus the mean annual ground surface temperature (MAGST) at a depth of 0.05 or 0.1 m. Although it is spatially variable depending on soil and temperature conditions, the magnitude of the thermal offset is small on the QTP compared with northern, high-latitude environments due to the prevalent coarse soil and low soil moisture content. The maximum thermal offset under natural conditions reported for the QTP is 0.79 °C (referenced as maximum thermal offset, TO_{max}) (Wu et al. , 2002; Wu et al., 2010; Lin et al, 2015). In this study, sites with MAGST + $TO_{max} \leqslant 0$ °C are considered to be permafrost sites. The reversed thermal offset reported on the QTP was not considered here because thermal offset measurements are not available for all sites, and the influence of the reversed thermal offset is expected to be minimal due to its small magnitude (the value was reported as -0.07 °C by Lin et al (2015))"

- P2, L31: What do you mean by clear? Can there be an opaque reflection? If the GPS survey is conducted in early summer, it could just be a measurement of the still frozen portion of seasonally frozen ground, rather than the active layer. This is why R#2 asked you to present criteria for the GPR surveys.
Response: Cao et al. (2017) gave a detailed description for GPR data acquisition and processing, I copied the sentences below:

  - Section 3 (P4): *GPR profiles with unexpected attenuation were removed before further analysis.*
  - Section 3.1.1 (P4): *Measurements were conducted with a MALÅ ProEX GPR by using 200 MHz and 100 MHz unshielded antennas from late September to November in 2014.*
  - Section 3.1.1 (P5): *During late September to October, the thaw depth reaches its maximum, and thus, ALT can be obtained (Wang et al. , 2016). In November, the near-surface soils have frozen, and at deeper layer, there is still an unfrozen layer with high amount of unfrozen water owing to the so-called "zero curtain" effect (maintaining temperatures close to the freezing point over extended periods of time in freezing or thawing soils.*

  This means (1) the opaque reflection was removed before further analysis, (2) GPR survey measured the active layer rather than seasonally frozen ground. We changed the sentence to

"GPR data are from Cao et al. (2017), and were measured in 2014 between late September and November using 100 and 200 MHz antennas. The GPR survey depth is from about 0.8 m to nearly 5 m depending on the active layer thickness. The data were carefully processed by removing opaque reflections, and evaluated using direct measurements. The ability of GPR data to detect permafrost relies on the strong dielectric contrast between liquid water and ice (Moorman et al., 2003). Consequently, it is more difficult to discern the presence of permafrost in areas with low soil moisture content because it weakens this contrast (Cao et al., 2017). For this reason, the GPR data were only considered to indicate the presence of permafrost if an active layer thickness

could be established."

to clarify.

- P3, L4: what is an arcsec? 3 arc second resolution?
  Response: Yes, it is the spatial resolution. the arcsec was changed to arc second(s) throughtout the manuscript. In this sentence, it is changed to
  "...a DEM with a spatial resolution of 3 arc second"

- P3, L8: Undefined "MAAT"
  Response: MAAT stands mean annual air temperature, and definition is added.

- P3, L18: neighbour?
  Response: Yes, it is changed to *"nearest-neighbour interpolation"* to clarify.

- P4, L4: add "PZI" before "map to allow..."
  Response: It is corrected as *"...into the PZI_{global} map..."*

- P4, L19: As stated, this is totally unrepeatable. Clearly state how you decided to aggregate the categorical map data. e.g., how do you reclassify sporadic permafrost?
  Response: Please see our responses to the major comment 2.

- P5, L7: "fair" to "slight" and "slight" to "poor"
  Response: The sentenec is changed to
  "...slight agreement for 0.2 $\kappa < 0:4$, and poor agreement for $\kappa < 0:2$."

- P6, L6: "showed underestimated" ???
  Response: "showed" was deleted.

- P6, L9: Please consider dividing this paragraph into a set according to map type.
  Response: This paragraph is divided as two parts, the categorical and the PZI map.

"Among the categorical maps, the QTP_{TTOP} map achieved the best performance for permafrost distribution over the QTP with the highest κ (0.58, moderate agreement) and PCC_{tol} (82.8%), however, caution should be taken when interpolating the map. The QTP_{TTOP} map was derived based on MODIS land surface temperature with temporal coverage of 2003–2012 (Zou et al., 2017). Though the MODIS land surface temperature time-series gaps caused mainly by clouds were filled using the Harmonic Analysis Time-Series (HANTS) algorithm (Prince et al., 1998), the surface conditions, especially vegetation and snow cover, were ignored. In this case, land surface temperature is underestimated in high or dense vegetation areas because it comes from the top of the vegetation canopy, and is overestimated in snow-covered areas where the cooling effects of snow are not considered. As a consequence, permafrost is likely overestimated in areas of high or dense vegetation and underestimated in regular snow covered areas. While the QTP_{Noah} map performed slightly better (2.5 % higher) for permafrost area than the QTP_{TTOP} map, it suffer from considerable underestimation of non-permafrost area (12.7% lower for PCC_{NPF}). Although the QTP_{Noah} map was derived using a coupled land surface model (Noah), the poorer performance, especially for non-permafrost area (PCC_{NPF} = 49.5%), is likely caused by the coarse-scale forcing dataset (0.1° resolution or ∼10 km) and by the uncertainty in the soil texture dataset (Chen et al., 2011; Yang et al., 2010). It is not surprising that the IPA map has slight agreement (κ = 0.21) because fewer observations were compiled and the methods used were more suitable for high latitudes (Ran et al., 2012).

For the PZI map, the PZI_{norm} and PZI_{cold} maps were found to be in moderate agreement (κ = 0.56 for the PZI_{norm} map and 0.55 for the PZI_{cold} map) with in-situ measurements, and performed slightly worse than the QTP_{TTOP} map. The poor performance of the PZI_{warm} map and underestimation of the PZI_{norm} map indicated that permafrost over the QTP is more prevalent than most of the other regions even though the climate conditions, especially the MAAT, are similar. This is likely because of the high soil thermal conductivity due to coarse soil and the cooling effects of minimal snow (Zhang, 2005). Large differences of permafrost region (0.42×10^6 km^2, or 25% of the normal case) and area (0.49×10^6 km^2, or 49% of the normal case) were found for the three cases of the PZI_{global} map, though the upper and lower bounds only changed about 5% for the PZI and ± 0.5 °C for the MAAT. The MAAT used in the PZI_{global} map was statistically downscaled from reanalysis based on the lapse rate derived from NCEP upper-air (pressure level) temperatures. The land surface influences on surface air temperature, such as cold air pooling, were ignored (Cao et al. , 2017). This is important as winter inversions are excepted to be common due to the prevalent mountains over the QTP. In other words, permafrost may be underestimated in valleys due to the overestimated MAAT."

Tables and Figures

Table 1

Not clear, poor writing: ”Criteria of continuous means permafrost distribution is compiled as PZI range of [0.01–1].”
Response: It is changed to
The continuous classification criteria means the permafrost spatial patterns is compiled or present as continuous value with a range of 0.01–1, e.g., permafrost zonation index in the PZI maps.

”Some bias is expected for permafrost areas of QTP_{TTOP} and QTP_{Noah} as different QTP boundaries, lake and glacier data are used.” is not really ”note” material. move to discussion.
Response: It is moved to discussion (P6, L25–26)

Table A1

I think that Table A1 should be included within the main document. If the writing is improved in this section, it and the information on page 7, lines 20-24, can be incorporated quite well.
Response: It is moved to the main text as Table 1 in the revised manuscript.

Figure 1

Response: (1) The legend was moved in frame (a); (2) slope aspect unit (°) was added in frame (c), and the north direction was marked; (3) the ylab was changed to *"$NDVI_{max}$"*; (4) all axis titles now begin with a Capital letter. The figure and caption were revised as below.

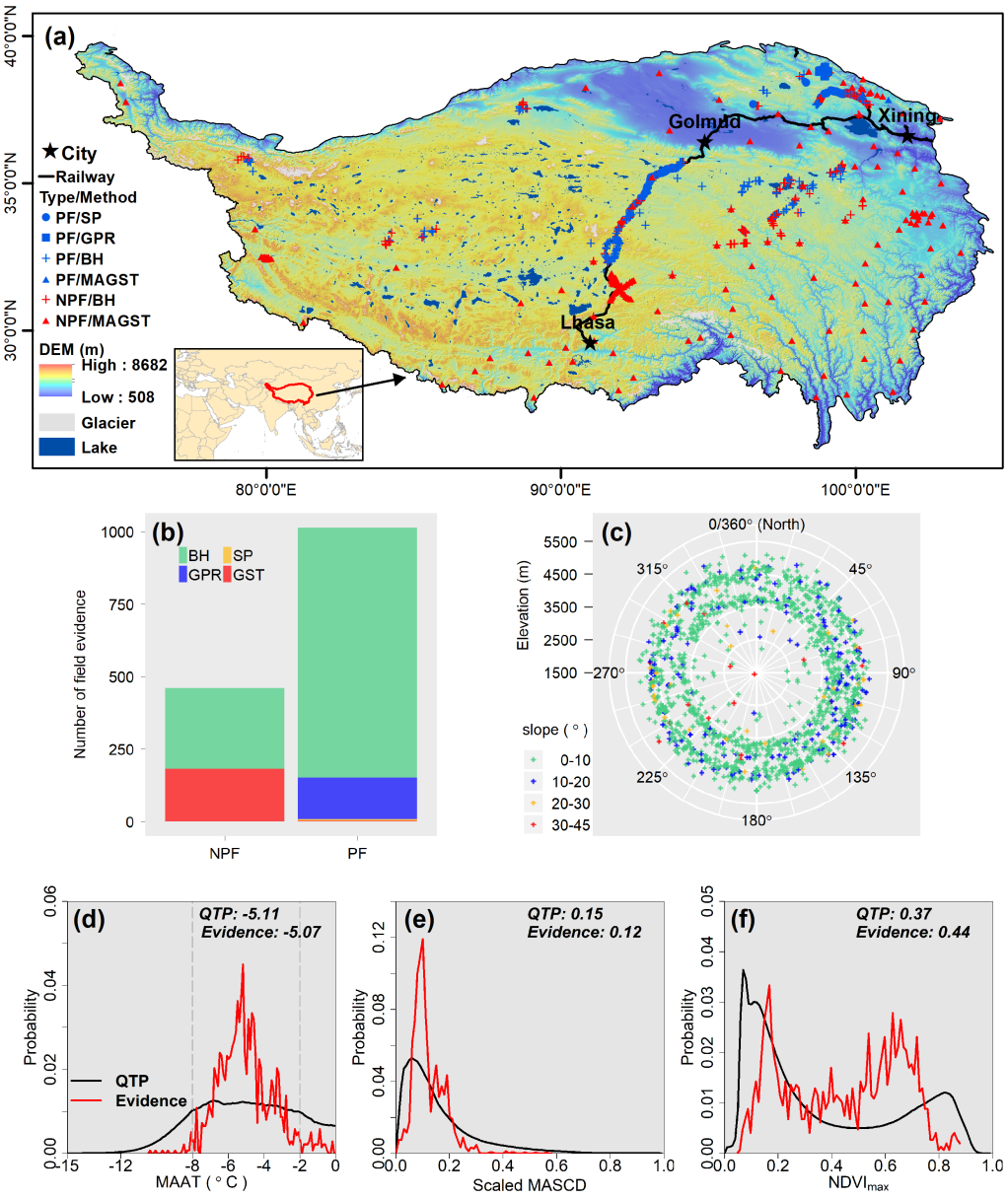

Figure 1: (a) The location of the QTP, and in-situ permafrost presence (PF) or absence (NPF) evidence distribution over the QTP, superimposed on the background of digital elevation model (DEM) with a spatial resolution of 30 arc second. (b) Number of field evidence located in NPF and PF regions. SP means soil pit, GPR means ground-penetrating radar, BH means field evidence measured by borehole drilling, and MAGST means mean annual ground surface temperature. (c) Distribution of field evidence in terms of elevation (radius), slope (colored), and aspect (0/360° represents North). Distributions of (d) with mean annual air temperature (MAAT), (e) scaled mean annual snow cover days (MASCD), and (f) annual maximum NDVI ($NDVI_{max}$) comparing to field evidence (red line) and the entire QTP (black line). Numbers in (d), (e), and (f) are mean values. Only the sites with MAAT < 0 °C, which is the precondition for permafrost presence, were present in (d).

Figure 2

Response:

- The city name and railway were removed from all frames;
- The Non-PF and PF were spelled out;
- PZI legend was merged in one line;
- The *PCC* description was removed from the caption.

The figure and caption were revised as below.

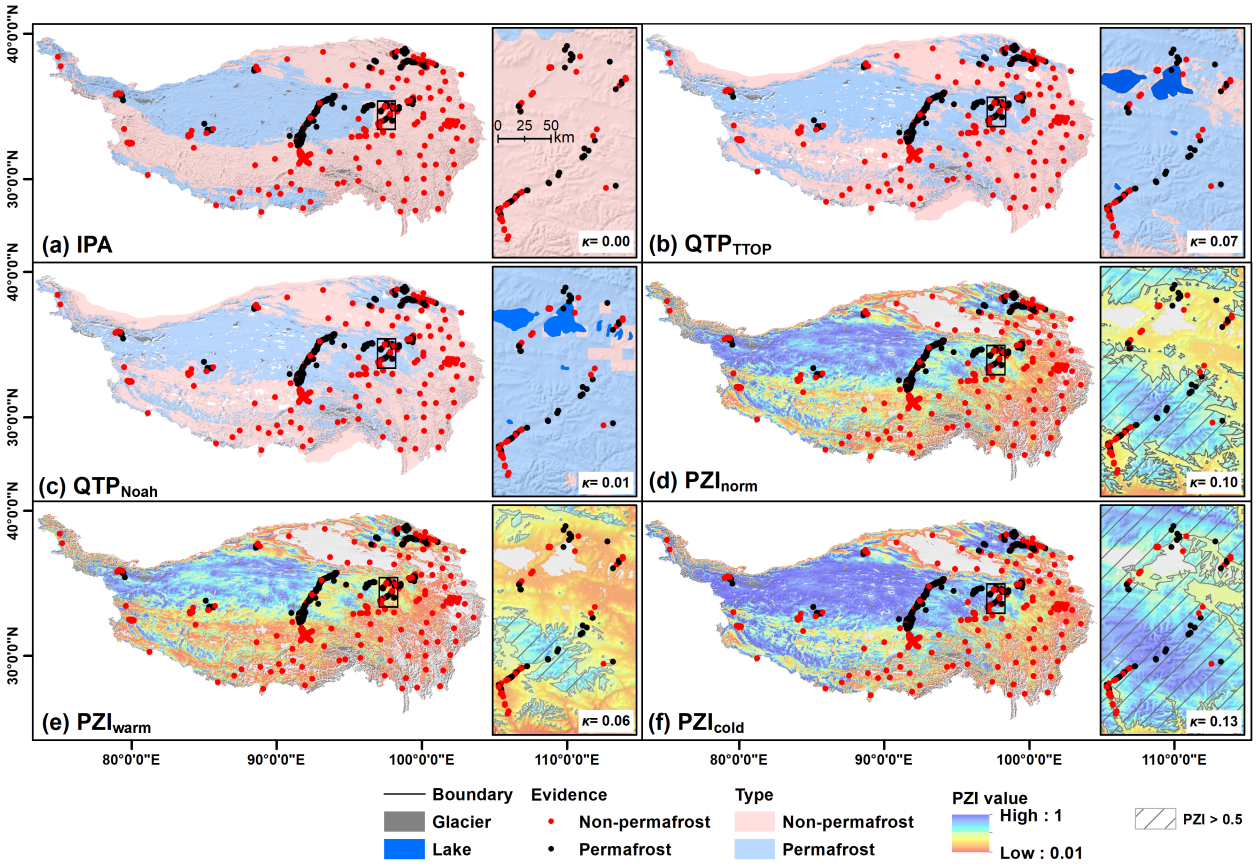

Figure 2: The permafrost classification results at in-situ evidence sites shown on the (a) IPA, (b) QTP_{TTOP}, (c) QTP_{Noah}, (d) PZI_{norm}, (e) PZI_{warm}, and (f) PZI_{cold} maps. The Cohen's kappa coefficient (κ), was derived from the selected spatially highly variable landscapes (marked by black box) with 106 evidence sites. All the maps are re-sampled to the unprojected grid of SRTM30 DEM with a spatial resolution of 30 arc second ($\sim$1 km) to avoid maps bias of with different resolutions, geographic projection, and format. The boundary of QTP used in this study is marked by black line. Categorical classification is used for tne QTP_{TTOP}, QTP_{Noah}, and IPA maps, while continuous PZI was present for the PZI_{norm}, PZI_{warm}, PZI_{cold} maps. The blank parts in the PZI maps are areas with PZI < 0.01.

References

Azócar, G. F., Brenning, A., & Bodin, X.: Permafrost distribution modelling in the semi-arid Chilean Andes, The Cryosphere, 11, 877–890, https://doi.org/10.5194/tc-11-877-2017, 2017.

Boeckli, L., Brenning, A., Gruber, S., and Noetzli, J.: Permafrost distribution in the European Alps: calculation and evaluation of an index map and summary statistics, The Cryosphere, 6, 807–820, https://doi.org/10.5194/tc-6-807-2012, 2012.

Cao, B., Gruber, S., and Zhang, T.: REDCAPP (v1.0): Parameterizing valley inversions in air temperature data downscaled from re-analyses, Geoscientific Model Development Discussions, 1–35. https://doi.org/10.5194/gmd-2017-60, 2017.

Cao, B., Gruber, S., Zhang, T., Li, L., Peng, X., Wang, K., Zheng, L., Shao, W., and Guo, H.: Spatial variability of active layer thickness detected by ground-penetrating radar in the Qilian Mountains, Western China, Journal of Geophysical Research: Earth Surface, https://doi.org/10.1002/2016JF004018, 2017.

Chen, Y., Yang, K., He, J., Qin, J., Shi, J., Du, J., & He, Q.: Improving land surface temperature modeling for dry land of China, Journal of Geophysical Research Atmospheres, 116(20), 1–15. https://doi.org/10.1029/2011JD015921, 2011.

Cremonese, E., Gruber, S., Phillips, M., Pogliotti, P., Boeckli, L., Noetzli, J., Noetzli, J., Suter, C., Bodin, X., Crepaz, A., Kellerer-Pirklbauer, A., Lang, K., Letey, S., Mair, V., Morra di Cella, U., Ravanel, L., Scapozza, C., Seppi, R Kellerer-Pirklbauer, A.: Brief Communication: An inventory of permafrost evidence for the European Alps, The Cryosphere, 5, 651–657. https://doi.org/10.5194/tc-5-651-2011, 2011

Gruber, S.: Derivation and analysis of a high-resolution estimate of global permafrost zonation, The Cryosphere, 6, 221–233. https://doi.org/10.5194/tc-6-221-2012, 2012.

Lin, Z., Burn, C. and Niu, F., Luo, J., Liu, M., and Yin, G.: The Thermal Regime, including a Reversed Thermal Offset, of Arid Permafrost Sites with Variations in Vegetation Cover Density, Wudaoliang Basin, Qinghai-Tibet Plateau, Permafrost and Periglacial Processes, 26(12): 142–159, 2015.

Moorman, B. J., Robinson, S. D., and Burgess, M. M.: Imaging periglacial conditions with ground-penetrating radar, Permafrost and Periglacial Processes, 14(4):319–329, https://doi.org/10.1002/ppp.463, 2003.

Prince, S. D., Goetz, S. J., Dubayah, R. O., Czajkowski, K. P., & Thawley, M.: Inference of surface and air temperature, atmospheric precipitable water and vapor pressure deficit using advanced very high-resolution radiometer satellite observations: Comparison with field observations, Journal of Hydrology, 212–213(1–4), 230–249. https://doi.org/10.1016/S0022-1694(98)00210-8, 1998.

Ran, Y., Li, X., Cheng, G., Zhang, T., Wu, Q., Jin, H., & Jin, R.: Distribution of Permafrost in China: An Overview of Existing Permafrost Maps, Permafrost and Periglacial Processes, 23(4), 322–333. https://doi.org/10.1002/ppp.1756, 2012.

Wu, J., Sheng, Y., Wu, Q., and Wen, Z.: Processes and modes of permafrost degradation on the Qinghai-Tibet Plateau, Science in China Series D: Earth Sciences, 35(1): 150–158, 2010.

Wu, Q., Zhu, Y., and Liu, Y.: Application of the Permafrost Table Temperature and Thermal Offset Forecast Model in the Tibetan Plateau, Journal of Glaciology and Geocryology, 24(5):24–27, 2002

Wang, Q., Zhang, T., Jin, H., Cao, B., Peng., X., Kang, W., Li, L., Guo, H., Liu, J., Cao, L.: Observational study on the active layer freeze–thaw cycle in the upper reaches of the Heihe River of the north-eastern Qinghai-Tibet Plateau. Quaternary International, 440:13–22, https://doi.org/10.1016/j.quaint.2016.08.027, 2016.

Yang, K., He, J., Tang, W., Qin, J., and Cheng, C. C. K: On downward shortwave and longwave radiations over high altitude regions: Observation and modeling in the Tibetan Plateau, Agricultural and Forest Meteorology, 150(1), 38–46. https://doi.org/https://doi.org/10.1016/j.agrformet.2009.08.004, 2010.

Zhang, T.: Influence of the seasonal snow cover on the ground thermal regime: An overview, Reviews of Geophysics, 43(4), 10.1029/2004RG000157, 2005.

Zou, D., Zhao, L., Sheng, Y., Chen, J., Hu, G., Wu, T., Wu, J., Xie, C., Wu, X., Pang, Q., Wang, W., Du, E., Li, W., Liu, G., Li, J., Qin, Y., Qiao, Y., Wang, Z., Shi, J., Cheng, G.: A new map of permafrost distribution on the Tibetan Plateau, The Cryosphere, 11(6), 2527–2542. https://doi.org/10.5194/tc-11-2527-2017, 2017.

Brief Communication: Evaluation and inter-comparisons of ~~permafrost map over the~~ Qinghai-Tibet Plateau permafrost maps based on a new inventory of ~~in-situ~~ field evidence

Bin Cao[1,2], Tingjun Zhang[1], Qingbai Wu[3], Yu Sheng[3], Lin Zhao[4], and Defu Zou[5]

[1]Key Laboratory of Western China's Environmental Systems (Ministry of Education), College of Earth and Environmental Sciences, Lanzhou University, Lanzhou 730000, China
[2]Department of Geography & Environmental Studies, Carleton University, Ottawa K1S 5B6, Canada
[3]State Key Laboratory of Frozen Soil Engineering, Cold and Arid Regions Environmental and Engineering Research Institute, Chinese Academy of Sciences, Lanzhou 730000, China
[4]School of Geographical Sciences, Nanjing University of Information Science and Technology, Nanjing 210044, China
[5]Cryosphere Research Station on the Qinghai-Tibet Plateau, State Key Laboratory of Cryospheric Science, Cold and Arid Regions Environmental and Engineering Research Institute, Chinese Academy of Sciences, Lanzhou 730000, China

Correspondence: Tingjun Zhang (tjzhang@lzu.edu.cn)

Abstract. Many maps have been produced to estimate permafrost distribution over the Qinghai-Tibet Plateau (QTP), ~~however, the estimated permafrost region (1.42–1.84×10^6 km^2) and area (0.76–1.25×10^6 km^2) are extremely large. The evaluation and inter-comparisons of~~ but the errors and biases among them are poorly understood due to limited ~~evidence. Using a large number data from various sources, we present the~~ field evidence. Here we evaluate and inter-compare the results of 6 different QTP permafrost maps against a new inventory of permafrost presence/absence ~~with~~ comprising 1475 ~~sites/plots over the QTP~~field sites compiled from various sources. Based on the in-situ measurements, our evaluation results showed a wide range of map performance with the Cohen's kappa coefficient from ~~0.32~~ 0.21 to 0.58 and overall accuracy between about 55–83%. The low agreement in areas near permafrost boundary and spatially highly variable landscapes ~~require improved method considering~~ highlights the need for improved mapping methods that consider more controlling factors at both medium-large and local scales.

1 Introduction

Permafrost is one of the major components of the cryosphere due to its large spatial extent. The Qinghai-Tibet Plateau (QTP), known as the Third Pole, has the largest extent of permafrost in the low-middle latitudes. Permafrost over the QTP was reported to be sensitive to ~~global warming~~ climate change mainly due to high ~~temperature (<~~ ground temperature (> -2 °C) (Wu and Zhang, 2008), and its distribution has strong influences on hydrological processes (e.g., ~~Cheng and Jin (2013)~~ Cheng and Jin, 2013; Zhang et al., 2018), biogeochemical processes (e.g., ~~Mu et al. (2017)~~Mu et al., 2017), and human systems (e.g., ~~Wu et al. (2016)~~Wu et al., 2016).

Many ~~maps have been produced to estimate~~ approaches have been used to produce permafrost distribution and ground ice ~~conditions~~ condition maps at different scales over the QTP (Ran et al., 2012). Typically, ~~frozen ground is classified~~ these maps

classify frozen ground into permafrost and seasonally frozen ground, and information on the extent, ~~i.e.~~ such as the areal abundance, of permafrost is available for some of ~~the maps~~ them (Ran et al., 2012). These maps significantly improved the understanding of permafrost distribution over the QTP~~, however,~~ . However, limited in-situ measurements and the different classification systems ~~as well as~~ and compilation approaches used make ~~the comparison of maps a challenge~~it challenging to compare maps directly. With the availability of high-resolution spatial data sets (e.g., surface air temperature and land surface temperature), several empirical and (semi-) physical models ~~are now~~ have been applied in permafrost distribution simulations at fine scales ~~(Nan et al., 2013; Zhao et al., 2017; Zou et al., 2017; Wu et al., 2018).Additionally, the QTP was involved~~ (e.g., Nan et al., 2013; Zhao et al., 2017; Zou et al., 2017; Wu et al., 2018). The QTP has also been included in hemispheric or global maps ~~, e.g.,~~ including the Circum-Arctic Map of Permafrost and Ground-ice Conditions ~~leaded~~ produced by the International Permafrost Association (referenced as IPA map) (Brown, 1997), and the global permafrost zonation index (PZI) map (referenced as PZI_{global} map) derived by Gruber (2012).

Despite the increasing efforts ~~made on permafrost mapping , existing maps over the QTP so far~~ in mapping QTP permafrost, the maps have not been evaluated and inter-compared with ~~large data sets. A large~~ the large amount of permafrost presence/absence evidence~~has been collected using a wide variety of methods (e.g., ground temperature~~ . These data have been collected since the 2000s, and represent a number of different field techniques including ground temperature measurements, soil pits, and geophysics~~) on the QTP since the 2000s. The new larger dataset can be used to improve evaluations~~ . A new inventory of this field evidence provides an opportunity to improve the evaluation of the existing ~~datasets, which would further improve their applications in permafrost~~ permafrost maps. This is an important step in describing the current body of knowledge on permafrost mapping performance as well as identifying any possible bias. It is also critical for identifying priorities when updating these maps in the future. Additionally, an improved evaluation is a useful guide to selecting a map to use for permafrost and related studies, ~~e.g.,~~ for example as a boundary condition for eco-hydrological model simulations. ~~The global warming and increasing amount of infrastructure built~~ Climate change and increasing infrastructure construction on permafrost add both environmental and engineering relevance to investigating permafrost distribution, and ~~makes studies~~ increase the importance of evaluating and comparing existing permafrost maps~~of great importance~~.

In this study, we aim to

1. ~~to~~ provide the first inventory of permafrost presence/absence evidence for the QTP; and
2. use the inventory to evaluate and inter-compare existing permafrost maps on the QTP~~, using the new inventory data~~.

2 Data and methods

2.1 Inventory of permafrost presence/absence evidence

Four methods ~~, including borehole temperature~~ were used to acquire evidence of permafrost presence or absence: borehole temperatures (BH), soil ~~pit~~ pits (SP), ground surface ~~temperature~~ temperatures (GST), and ground-penetrating radar (GPR) ~~survey, were used to acquire evidence of permafrost presence or absence~~ surveys (Figure 1, Table1). In this study, we used

the mean ~~annual~~ ground temperature (~~MAGT~~MGT) measured from ~~borehole,~~ the borehole, the depth of which varies from meters to about 20 m depending on the depth of zero annual amplitude and borehole depth, to identify permafrost presence or absence. Due to the ~~prevalent~~ prevalence of coarse soil, ~~SP was only applied in areas possible, and the depth is~~ there are only 6 SP sites and the depths range from less than 1 ~~meter~~ m to about 2.5 m. ~~GST, referred as soil~~ Thermal offset is defined as the mean annual temperature at the ~~depth of 0.05 or 0.1 m here, was used to establish permafrost presence/absence for specific sites due to the MAGT could be derived as the difference of thermal offset and~~ top of permafrost (TTOP) minus the mean annual ground surface temperature (MAGST) ~~(Hasler et al., 2015). While thermal offset~~ at a depth of 0.05 or 0.1 m. Although it is spatially variable depending on soil and temperature conditions, ~~it is relatively~~ the magnitude of the thermal offset is small on the QTP compared with northern~~high latitudes~~, high-latitude environments due to the prevalent coarse soil and low soil moisture content. The maximum thermal offset under natural conditions reported for the QTP is 0.79 °C (referenced as maximum thermal offset, TO_{max}) (Wu et al., 2002, 2010; Lin et al., 2015). In this study, sites with $MAGST + TO_{max} \leqslant 0$ °C are considered ~~as~~ to be permafrost sites. The ~~suitability of GPR for detecting permafrost derives from the dielectric contrast between liquid water and ice (Moorman et al., 2003), and it may face the challenge of distinguishing presence of permafrost in areas with low soil moisture content (Cao et al., 2017b). Here, GPR data from Cao et al. (2017b) are measured~~ reversed thermal offset reported on the QTP was not considered here because thermal offset measurements are not available for all sites, and the influence of the reversed thermal offset is expected to be minimal due to its small magnitude (the value was reported as -0.07 °C by Lin et al. (2015)). GPR data are from Cao et al. (2017b), and were measured in 2014 between late September and November using 100 and 200 MHz antennas~~depending on the active layer thickness~~. The GPR survey depth is from about 0.8 ~~to near~~ m to nearly 5 m ~~, and~~ depending on the active layer thickness. The data were carefully processed by removing opaque reflections, and evaluated using direct measurements. The ability of GPR data to detect permafrost relies on the strong dielectric contrast between liquid water and ice (Moorman et al., 2003). Consequently, it is more difficult to discern the presence of permafrost in areas with low soil moisture content because it weakens this contrast (Cao et al., 2017b). For this reason, the GPR data were only considered to indicate the ~~data are considered as indicating the~~ presence of permafrost ~~only~~ if an active layer thickness ~~(or a clear permafrost reflection)~~ could be established.~~The detailed classification algorithm of in-situ~~

In order to apply the permafrost presence or absence ~~evidence could be found from Appendix A.~~ inventory more broadly, the degree of confidence in the data is estimated and provided in the inventory and in Table 1, although it is not used in this study. BH and SP provide direct evidence of permafrost presence or absence based on MGT and/or ground ice observations, and hence have high confidence (Cremonese et al., 2011). The data confidence derived from MAGST is classified based on temperature and the length of the observation period. The evaluated GPR survey result was considered to have medium confidence.

2.2 Topographical and climatological properties of the inventory sites

The slope and aspect ~~of the inventory~~ for the inventory sites were derived from a DEM with 3 ~~arcsec~~arc second spatial resolution, which is aggregated from the Global Digital Elevation Model version 2 (GDEM2) by averaging to avoid the noise in the original dataset (Cao et al., 2017a). The thermal state ~~of permafrost and its spatial distribution~~ and spatial distribution of permafrost result from the long-term interaction of the climate and subsurface. Additionally, vegetation and snow ~~coverage~~

cover play important roles in permafrost distribution ~~through~~ by influencing the energy exchange between the atmosphere and the ground surface (Norman et al., 1995; Zhang, 2005). In this study, three climate variables ~~of MAAT~~were selected to test the representativeness of the inventory for permafrost map evaluation: mean annual air temperature (MAAT), mean annual snow cover days (MASCD), and the annual maximum normalized difference vegetation index (NDVI~~) were hence selected here to test the representative of the inventory for permafrost map evaluation~~$_{max}$). The MAAT ~~with~~ was obtained from Gruber (2012), it has a spatial resolution of 1 km ~~is from Gruber (2012) representing the referenced period~~ and represents the reference period spanning 1961–1990. The MASCD, with a spatial resolution of about 500 m, was derived from a daily snow cover product developed by Wang et al. (2015) based on MODIS products (MOD10A1 and MYD10A1). To improve the comparison of MASCD, it ~~is scaled to 0–1 through~~ was scaled to values between 0 and 1 by dividing the total days of a given year, and the mean MASCD during 2003–2010 was produced as a predictor. The annual maximum NDVI is from the MODIS/Terra ~~Vegetation Indices~~ 16-day Vegetation Index product (MOD13Q1, v006) ~~with a~~ which has a spatial resolution of 250 m. ~~The annual maximum NDVI (NDVI$_{max}$)~~ It was computed for each year ~~during~~ between 2001–2017 to ~~approximately represent the~~ represent the approximate amount of vegetation, and then aggregated ~~as a median~~ to a median value for the entire period to avoid sensitivity to extreme values. These climate variables were extracted ~~to in-situ sites based on nearest~~ for field site locations based on nearest-neighbor interpolation. The outline of the QTP is from Zhang et al. (2002), glacier outlines ~~is~~ are from Liu et al. (2015) representing conditions in 2010, and lake data is provided by the Third Pole Environment Database.

2.3 Existing maps over the QTP

Table 2 gives ~~the summary of~~ a summary of the most widely used and ~~recent~~ recently developed permafrost maps over the QTP. In general, permafrost maps over the QTP could be classified as: (i) categorical, using categorical classification with different permafrost ~~types~~ categories (e.g., continuous, discontinuous, sporadic, and island permafrost), ~~seasonally frozen ground, and unfrozen ground, and~~ or (ii) continuous, using a continuous probability or ~~indices~~ index with a range of [~~0–1~~0.01–1] to represent the proportion of an area that is underlain by permafrost. The IPA map, which ~~is may~~ may be the most widely used categorical map, was ~~complied~~ compiled by assembling all readily available data on the characteristics and distribution of permafrost (Ran et al., 2012). The IPA map uses the "permafrost zone" to describe spatial patterns of permafrost, and the areas are divided into five categories based on the proportion of the ground underlain by permafrost: continuous (> 90%), discontinuous (50–90%), sporadic (10–50%), island (0–10%) and absent (0%). The most recent efforts were made by Zou et al. (2017) using the ~~mean annual temperature at the top of permafrost (TTOP)~~ TTOP model (referenced as QTP$_{TTOP}$ map) forced by a calibrated (using station data) land surface temperature (or freezing and thawing indices) considering soil properties, and by Wu et al. (2018) based on the Noah land surface model (referenced as QTP$_{Noah}$ map) as well as gridded meteorological ~~dataset~~datasets, including surface air temperature, radiation, and precipitation. ~~Though,~~ Although these two categorical maps are expected to be superior ~~by using~~ because they use the latest measurements and advanced methods, they were evaluated using limited and narrow distributed data (∼200 sites for the QTP$_{TTOP}$ map and 56 sites for the QTP$_{Noah}$ map). The PZI$_{global}$ map, which gives ~~continuous index~~ a continuous index value for permafrost distribution, is derived through ~~its~~ a heuristic-empirical relationship with mean annual air temperature (MAAT) based on generalized linear models (Gruber, 2012). The model parameters are established

largely based on the boundaries of continuous (PZI = 0.9 for MAAT = -8.0 °C) and ~~isolated~~ island (PZI = 0.1 for MAAT = -1.5 °C) permafrost in the IPA map and do not use field observations. ~~Additionally, two cases, including~~ Gruber (2012) introduced two end-member cases for either cold (conservative or more permafrost) ~~and warm (anti-conservative~~ or warm (non-conservative or less permafrost) ~~, were introduced into the~~ conditions, into the PZI_{global} map to allow the propagation of uncertainty caused by input ~~dataset~~ datasets and model suitability. The three cases or maps, referenced as PZI_{norm}, PZI_{warm}, and PZI_{cold} maps, differ in the parameters used. ~~Comparing~~ Compared to the normal case, the cold and warm variants are derived by shifting PZI and MAAT at the respective limit by $\pm$ 5% and $\pm$ 0.5 °C, respectively. The PZI_{global} map was partly evaluated for the QTP using rock glaciers, considered as indicators of permafrost conditions, based on remote sensing imagery (Schmid et al., 2015). ~~Rock glaciers, however are of absence~~ However, rock glaciers, are absent in much of the QTP due to very low precipitation (Gruber et al., 2017).

2.4 Statistics and evaluation of permafrost distribution maps

In ~~this study~~order to compare maps, it is important to understand the difference between extent of permafrost ~~region~~ regions and permafrost area. Permafrost ~~region refers to regions where permafrost exists but the entire region is not necessarily completely occupied~~ area refers to the quantified extent of area within a domain that is completely underlain by permafrost, ~~while permafrost area refers to areas where are completely~~ whereas permafrost regions are categorical areas within a domain that are defined by the percent of land area underlain by permafrost. For example, ~~discontinuous permafrost regions have permafrost area ranging from~~ extensive discontinuous permafrost is a region where, by definition, 50 to 90% of the land area is underlain by permafrost. In other words, in discontinuous permafrost region, there 50 to 90% of the area is underlain by permafrost, i.e., permafrost area ~~(Zhang et al., 2000; Gruber, 2012). To estimate permafrost region and area based on the PZI as model output,~~ (Zhang et al., 2000).

To conduct the map evaluations against measurements with binary information (presence or absence), it was necessary to develop classification aggregations for the existing maps. We argue that although the aggregation presented here simplifies the information available in these maps and may introduce uncertainty for further analyses, it is necessary in order to conduct inter-comparisons among them. For the IPA map, we consider the continuous and discontinuous permafrost zones to correspond to permafrost presence and the other zones (sporadic permafrost, island permafrost, and non-permafrost) to correspond to permafrost absence by using the proportion of ground underlain by permafrost of 50% as a threshold. This is consistent with the threshold of the PZI map described below. For the QTP_{TTOP} and QTP_{Noah} maps, the permafrost distribution was derived using simulated mean annual ground temperature (thermally defined). In these maps, areas are classified into three type: permafrost, seasonally frozen ground, and unfrozen ground. Here, we merge the areas of seasonally frozen ground and unfrozen ground to yield areas of permafrost absence. For the PZI maps, specified thresholds are required for both the extent of permafrost region and permafrost area. ~~By following~~ Following Gruber (2012), only the areas with PZI $\geq$ 0.01 were selected for further analysis, permafrost ~~region is defined as the area with~~ regions were defined as where PZI $\geq$ 0.1, and permafrost area was ~~derived~~ calculated as PZI multiplied pixel area. A value of 0.5 was used as the threshold of permafrost presence and absence (Boeckli et al., 2012; Azócar et al., 2017).

~~For map evaluation, the categorical map was aggregated to binary by merging different permafrost types as permafrost presence 1and by merging the others as permafrost absence 0. Evaluations of the maps are conducted using classification accuracies~~ Maps were evaluated based on field evidence to produce accuracy measurements as follows (Wang et al., 2015) :

$$PCC_{PF} = \frac{PF_T}{PF_T + PF_F} \times 100\% \tag{1}$$

$$PCC_{NPF} = \frac{NPF_T}{NPF_T + NPF_F} \times 100\% \tag{2}$$

$$PCC_{tol} = \frac{PF_T + NPF_T}{PF_T + PF_F + NPF_T + NPF_F} \times 100\% \tag{3}$$

where ~~subscripts of T (True, correctly classified) and F (False, incorrectly classified) identify corrections of classification. In this case,~~ PF_T is ~~permafrost presence sites /plots~~ the number of permafrost sites correctly classified as permafrost, while PF_F is the number of permafrost sites incorrectly classified as non-permafrost. Similarly, NPF_T is ~~permafrost absence~~ the number of permafrost-absent sites correctly classified as non-permafrost, and NPF_F is ~~incorrectly classified as permafrost~~the number of incorrectly classified non-permafrost sites. PCC is ~~percent of sites /plots~~ the percentage of sites correctly classified, and the subscripts ~~of~~ PF, NPF, and tol ~~means~~ indicate permafrost, non-permafrost, and total sites~~/plots~~, respectively. ~~For the PZI map, the PZI of 0.5 was used as the threshold of permafrost presence and absence (Boeckli et al., 2012; Azócar et al., 2017), and the above index were tested.~~ To avoid the impact of ~~uneven distribution of sample numbers for permafrost~~ unequal sample sizes in each of the two categories (presence and absence), the Cohen's kappa coefficient (κ), which measures inter-rater agreement for categorical items (Landis and Koch, 1977), was ~~introduced here~~ used for map evaluation~~.~~ :

$$\kappa = \frac{p_o - p_e}{1 - p_e} \tag{4}$$

where p_e and p_o are the probability of random agreement and disagreement, respectively, and can be calculated as

$$p_e = \frac{(PF_T + PF_F) \times (PF_T + NPF_F)}{(PF_T + PF_F + NPF_F + NPF_T)^2} \tag{5}$$

$$p_o = \frac{(NPF_F + NPF_T) \times (PF_F + NPF_T)}{(PF_T + PF_F + NPF_F + NPF_T)^2} \tag{6}$$

Cohen's kappa coefficient ~~result is interpreted as~~ results are interpreted to mean excellent agreement for ~~$k \geqslant 0.8$~~$\kappa \geqslant 0.8$, substantial agreement for ~~$0.6 \leqslant k < 0.8$~~$0.6 \leqslant \kappa < 0.8$, moderate agreement for ~~$0.4 \leqslant k <$~~ $0.4 \leqslant \kappa <$ 0.6, ~~fair agreement for $0.2 \leqslant k < 0.4$, and~~ slight agreement for ~~$k < 0.2$~~$0.2 \leqslant \kappa < 0.4$, and poor agreement for $\kappa < 0.2$.

3 Results and discussion

3.1 Evidence of Permafrost Presence or Absence

There are ~~in total~~ a total of 1475 permafrost presence or absence sites ~~/plots~~ contained in the inventory acquired from BH, SP, GST, and GPR methods (Figure 1). Among ~~the 1475 evidences, there are~~ these, 1141 (77.4%) sites were measured by BH, 184

(12.5%) sites by GST, 144 (9.8%) ~~plots~~ sites by GPR, and 6 (0.4%) sites by SP (Figure 1b). There are 1012 (68.6%) permafrost presence sites ~~/plots~~ and 463 (31.4%) permafrost absence sites~~/plots. These evidences extend over~~ . The data cover a large area of the QTP (latitude: 27.73–38.96°N, longitude: 75.06–103.57°E) (Figure 1c) ~~. The evidence cover~~ and a wide elevation range from about 1600 m to ~~over~~ above 5200 m~~, however, the majority~~ . However, the majority of sites (93.2%) ~~is~~ are located between 3500 m and 5000 m. ~~While the inventory showed~~ The inventory has an even distribution of aspects with 27.3% on the east slope, 27.9% on the south slope, 22.0% on the west slope, and 22.6% on the north slope~~, most of the evidence~~ . Most of the sites (96.1%) have slope angles less than 20° (Figure 1c).

Figure 1d, e~~and f present the coverage of evidence for selected climate variables , which could significantly influence permafrost distribution~~, and f compare the distribution of three climate variables between the field sites and the entire QTP. The 1475 field sites ~~/plots showed a relatively~~ have a narrower MAAT range (-10.5–15.7 °C with Q25 lower quantile = -6.0 °C and Q75 upper quantile = -3.8 °C) ~~comparing~~ compared to the entire QTP ~~with~~ which has a MAAT between -25.6 and 22.1 °C (Q25 lower quantile = -6.6 °C and Q75 upper quantile = -0.41 °C), and only 1.5% sites ~~/plots~~ located in the area with MAAT $<$ -8 °C. However, the ~~evidence~~ data (88.2%) ~~was mainly occurred~~ were mostly found in the most sensitive MAAT range (from -8 to -2 °C) ~~of permafrost presence /absence changing with MAAT~~ for permafrost presence or absence (Gruber, 2012; Cao et al., 2018). There is a slight bias ~~for~~ in the scaled MASCD coverage~~with little~~ . Few measurements (7.5%) ~~in~~ were located in areas of high scaled MASCD ($>$ 0.20) ~~area~~ due to the associated harsh climate and inconvenient access. The ~~annual maximum NDVIat evidence sites/plots has~~ $NDVI_{max}$ at field evidence sites have a wide coverage for the QTP with the range of 0.05–0.88. The higher mean NDVI~~for evidence~~$_{max}$ for field sites (0.44 at the sample sites ~~/plots~~ and 0.37 for the QTP) is due to the ~~measurements are occurred~~ fact that measurements were normally collected in flat areas with relatively dense vegetation cover. ~~The exploration of inventory indicated~~ These results suggest that the evaluation presented in this study ~~to be representative for~~ are representative of most of the QTP ~~, and may have pronounced~~ but may have more uncertainty in steep and ~~regular~~ regularly snow-covered regions.

3.2 Evaluation and comparison of existing maps

The new inventory was used to evaluate existing permafrost maps derived with different methods (Table 2). In general, these permafrost maps showed different performances, including slight agreement for the IPA map, fair agreement for the PZI_{warm} ~~and IPA maps~~map, moderate agreement for the QTP_{Noah}, PZI_{norm}, PZI_{cold}, and QTP_{TTOP} maps, with a wide spread of κ from ~~0.32~~ 0.21 to 0.58. The high PCC_{PF} together with low PCC_{NPF} for the ~~IPA,~~ QTP_{Noah}, PZI_{cold}, and QTP_{TTOP} maps indicate permafrost is ~~over-presented~~ overestimated by them, while the ~~PZI_{warm}~~ IPA, PZI_{warm}, and PZI_{norm} maps ~~showed~~ underestimated the permafrost over the QTP. ~~Additionally,~~ Despite the small permafrost area bias for the QTP_{TTOP} and QTP_{Noah} maps caused by different QTP boundaries, lake, and glacier datasets used, the range of estimated permafrost region (1.42–1.84 $\times$ 10^6 km^2, or 30% difference) and area (0.76–1.25 $\times$ 10^6 km^2, or 64.4% difference) are extremely large (Figure 2).

~~The~~ Among the categorical maps, the QTP_{TTOP} map achieved the best performance for permafrost distribution over the QTP with the highest κ (0.58, moderate agreement) and PCC_{tol} (82.8%), however, ~~patience~~ caution should be taken ~~to interpolate~~ when interpolating the map. The QTP_{TTOP} map was derived based on MODIS land surface temperature with ~~different~~ tempo-

ral coverage of 2003–2012 (Zou et al., 2017). Though the MODIS land surface temperature time-series gaps caused mainly by ~~cloud~~ clouds were filled using the Harmonic Analysis Time-Series (HANTS) algorithm (Prince et al., 1998), the surface conditions, especially vegetation and snow cover, were ignored. In this case, land surface temperature is underestimated in high ~~and/~~or dense vegetation ~~area as~~ areas because it comes from the top of the vegetation canopy, and is overestimated in snow-covered ~~area due to~~ areas where the cooling effects of snow ~~is~~ are not considered. As a consequence, permafrost is likely overestimated in ~~high and/~~areas of high or dense vegetation ~~area~~ and underestimated in ~~regular snow covered area . The PZI~~ regularly snow-covered areas. While the QTP_{Noah} map performed slightly better (2.5 % higher) for permafrost area than the QTP_{TTOP} map, it suffer from considerable underestimation of non-permafrost area (12.7% lower for PCC_{NPF}). Although the QTP_{Noah} map was derived using a coupled land surface model (Noah), the poorer performance, especially for non-permafrost area (PCC_{NPF} = 49.5%), is likely caused by the coarse-scale forcing dataset (0.1° resolution or ∼10 km) and by the uncertainty in the soil texture dataset (Chen et al., 2011; Yang et al., 2010). It is not surprising that the IPA map has slight agreement (κ = 0.21) because fewer observations were compiled and the methods used were more suitable for high latitudes (Ran et al., 2012)
.

For the PZI map, the PZI_{norm} and PZI_{cold} maps ~~, judged as~~ were found to be in moderate agreement (κ = 0.56 for the PZI_{norm} map and 0.55 for the PZI_{cold} map) with in-situ measurements, ~~showed slightly worse performance comparing with~~ and performed slightly worse than the QTP_{TTOP} map. The poor performance of the PZI_{warm} map and ~~understimation~~ underestimation of the PZI_{norm} map indicated that permafrost over the QTP is more prevalent than most of the other regions even ~~when~~ though the climate conditions, especially the MAAT, are similar. This is ~~very likely because~~ likely because of the high soil thermal conductivity due to coarse soil ~~conditions~~ and the cooling effects of minimal snow (Zhang, 2005). ~~Great difference~~ Large differences of permafrost region (0.42×10^6 km^2, or 25% of the normal case) and area (0.49×10^6 km^2, or 49% of the normal case) ~~was~~ were found for the three cases of the PZI_{global} map, though the upper and lower bounds ~~of MAAT are~~ only changed about 5% for the PZI and ± 0.5 °C for the MAAT. The MAAT used in the PZI_{global} map was ~~statistical downscaled~~ statistically downscaled from reanalysis based on the lapse rate ~~from the~~ derived from NCEP upper-air (~~or~~ pressure level) ~~temperature of NCEP, but the influences of land surface~~ temperatures. The land surface influences on surface air temperature, such as cold air pooling, ~~was~~ were ignored (Cao et al., 2017a). This is important as winter ~~inversion is~~ inversions are excepted to be common due to the prevalent mountains over the QTP. In other words, permafrost may be underestimated in valleys due to the overestimated MAAT.~~While the IPA and QTP_{Noah} maps performed slightly better (1.8–3.1% higher) for permafrost areas than the QTP_{TTOP} and PZI_{cold} maps, they suffer considerable underestimation of non-permafrost area (14.1–39.8% lower for PCC_{NPF}). Though the QTP_{Noah} map was derived using coupled land surface model (Noah), the relatively worse performance, especially for non-permafrost area (PCC_{NPF} = 49.5%), is likely caused by inputting coarse-scale forcing dataset (0.1° resolution or ∼10 km) (Chen et al., 2011) and by the uncertainty of soil texture dataset (Yang et al., 2010). It is not surprising that the IPA map has fair agreement (κ = 0.24) as less observations were compiled and the method used are more suitable for high latitudes (Ran et al., 2012).~~

Spatially, the ~~southeastern QTP of~~ non-permafrost areas ~~are better~~ of the southeastern QTP are well represented in all maps, while misclassification is prevalent in areas near the permafrost boundary and spatially highly variable landscapes such as the

sources of the Yellow River (Figure 2). This is because the permafrost ~~distribution~~ spatial patterns in these areas ~~is~~ are not only controlled by ~~medium-large scale~~ medium- to large-scale climate conditions (e.g., MAAT), which are described by the models used, but also strongly influenced by various local factors such as peat ~~layer~~layers, thermokarst, soil moisture, and hydrological processes. The IPA and PZI_{warm} maps showed a fit that is good only in some areas (e.g., ~~southeastern for the PZI_{warm} map and~~ relatively colder areas for the IPA map and southeastern for the PZI_{warm} map) based on the in-situ measurements, and may not represent the permafrost distribution patterns well for the other areas beyond the ~~measurement~~measurements.

4 Conclusions

We compiled an inventory of evidence for permafrost presence or absence ~~evidence with~~ using 1475 field sites ~~/plots~~ obtained based on diverse methods over the QTP. With a wide coverage of topography (e.g., elevation and slope aspect) and climate conditions (e.g., surface air temperature and snow cover), the inventory gives a representative baseline for site-specific permafrost occurrence.

The existing permafrost maps over the QTP were ~~better evaluated and compared with~~ evaluated and inter-compared using the inventory of ground-based evidence, and they showed a wide range of performance with the κ from ~~0.32~~ 0.21 to 0.58 and overall classification accuracy of about 55–83%. The QTP_{TTOP} map is recommended for representing permafrost distribution over the QTP based on our ~~evaluations~~evaluation. Additionally, the PZI_{norm} and PZI_{cold} maps ~~with close performance~~ similarly to one another and are valuable alternatives for describing a permafrost zonation index over the QTP. The inadequate sampling is expected to result in higher uncertainty for map evaluation in ~~steeps and regular~~ steep and regularly snow-covered areas, and requires further investigation using systematic samples.

Data availability. Inventory of permafrost presence/absence is partly available as supplement, the other evidence sites not listed are available from the authors upon request.

Appendix A: ~~Classification algorithm of in-situ permafrost presence or absence evidence~~

~~For board use of the permafrost presence or absence inventory, the data confidence degree was provided (Table1). BH and SP provide direct evidence of permafrost presence or absence based on MAGT and/or ground ice observations, and hence have high confidence (Cremonese et al., 2011). The data confidence derived from MAGST is classified based on temperature and the length of the observation period. The evaluated GPR survey result was considered as medium confidence.~~

Author contributions. BC carried out this study by organizing the inventory of permafrost presence or absence evidence, analyzing data, performing the simulations and by structuring as well as writing the paper. TZ guided the research. QW, YS, LZ, and DZ contributed to organize the permafrost presence/absence dataset.

Competing interests. The authors declare that no competing interests are present.

Acknowledgements. The authors would like to thank ~~Stephan Gruber~~ the Editor Peter Morse, two anonymous, Stephan Gruber, and Kang Wang for their constructive suggestions. We thank Nicholas Brown for improving the writing of earlier manuscript. We thank Zhuotong Nan and Xiaobo Wu for providing the QTP_{Noah} map. This study was supported by the Strategic Priority Research Program of Chinese Academy of Sciences (XDA20100103, XDA20100313), the National Natural Science Foundation of China (~~91325202), the National Key Scientific Research Program of China (2013CBA01802~~41871050, 41801028), partly by the Fundamental Research Funds for the Central Universities (lzujbky_2016_281, 862863). We thank CMA (http://cdc.cma.gov.cn/) for providing the surface air and ground surface temperatures, the ASTER dataset is downloaded from United States Geological Survey (http://gdex.cr.usgs.gov/gdex/), glacier inventory is provided by the Environmental and Ecological Science Data Center for West China (http://westdc.westgis.ac.cn/), and lake inventory is from the Third Pole Environment Database (http://www.tpedatabase.cn).

References

Azócar, G. F., Brenning, A., and Bodin, X.: Permafrost distribution modelling in the semi-arid Chilean Andes, The Cryosphere, 11, 877–890, https://doi.org/10.5194/tc-11-877-2017, 2017.

Boeckli, L., Brenning, A., Gruber, S., and Noetzli, J.: Permafrost distribution in the European Alps: calculation and evaluation of an index map and summary statistics, The Cryosphere, 6, 807–820, https://doi.org/10.5194/tc-6-807-2012, 2012.

Brown, J., F. J. O. H. J. M. E.: Circum-Arctic Map of Permafrost and Ground-ice Conditions, 1997.

Cao, B., Gruber, S., and Zhang, T.: REDCAPP (v1.0): parameterizing valley inversions in air temperature data downscaled from reanalyses, Geoscientific Model Development, 10, 2905–2923, https://doi.org/10.5194/gmd-10-2905-2017, 2017a.

Cao, B., Gruber, S., Zhang, T., Li, L., Peng, X., Wang, K., Zheng, L., Shao, W., and Guo, H.: Spatial variability of active layer thickness detected by ground-penetrating radar in the Qilian Mountains, Western China, Journal of Geophysical Research: Earth Surface, 122, 574–591, https://doi.org/10.1002/2016JF004018, 2016JF004018, 2017b.

Cao, B., Zhang, T., Peng, X., Mu, C., Wang, Q., Zheng, L., Wang, K., and Zhong, X.: Thermal Characteristics and Recent Changes of Permafrost in the Upper Reaches of the Heihe River Basin, Western China, Journal of Geophysical Research: Atmospheres, 123, 7935–7949, https://doi.org/10.1029/2018JD028442, https://agupubs.onlinelibrary.wiley.com/doi/abs/10.1029/2018JD028442, 2018.

Chen, Y., Yang, K., He, J., Qin, J., Shi, J., Du, J., and He, Q.: Improving land surface temperature modeling for dry land of China, Journal of Geophysical Research: Atmospheres, 116, https://doi.org/10.1029/2011JD015921, d20104, 2011.

Cheng, G. and Jin, H.: Permafrost and groundwater on the Qinghai-Tibet Plateau and in northeast China, Hydrogeology Journal, 21, 5–23, https://doi.org/10.1007/s10040-012-0927-2, https://doi.org/10.1007/s10040-012-0927-2, 2013.

Cremonese, E., Gruber, S., Phillips, M., Pogliotti, P., Boeckli, L., Noetzli, J., Suter, C., Bodin, X., Crepaz, A., Kellerer-Pirklbauer, A., Lang, K., Letey, S., Mair, V., Morra di Cella, U., Ravanel, L., Scapozza, C., Seppi, R., and Zischg, A.: Brief Communication: "An inventory of permafrost evidence for the European Alps", The Cryosphere, 5, 651–657, https://doi.org/10.5194/tc-5-651-2011, 2011.

Gruber, S.: Derivation and analysis of a high-resolution estimate of global permafrost zonation, The Cryosphere, 6, 221–233, https://doi.org/10.5194/tc-6-221-2012, 2012.

Gruber, S., Fleiner, R., Guegan, E., Panday, P., Schmid, M.-O., Stumm, D., Wester, P., Zhang, Y., and Zhao, L.: Review article: Inferring permafrost and permafrost thaw in the mountains of the Hindu Kush Himalaya region, The Cryosphere, 11, 81–99, https://doi.org/10.5194/tc-11-81-2017, 2017.

Hasler, A., Geertsema, M., Foord, V., Gruber, S., and Noetzli, J.: The influence of surface characteristics, topography and continentality on mountain permafrost in British Columbia, The Cryosphere, 9, 1025–1038, https://doi.org/10.5194/tc-9-1025-2015, 2015.

Landis, J. R. and Koch, G. G.: The Measurement of Observer Agreement for Categorical Data, Biometrics, 33, 159–174, http://www.jstor.org/stable/2529310, 1977.

Lin, Z., Burn, C. R., Niu, F., Luo, J., Liu, M., and Yin, G.: The Thermal Regime, including a Reversed Thermal Offset, of Arid Permafrost Sites with Variations in Vegetation Cover Density, Wudaoliang Basin, Qinghai-Tibet Plateau, Permafrost and Periglacial Processes, 26, 142–159, https://doi.org/10.1002/ppp.1840, 2015.

Liu, S., Yao, X., Guo, W., Xu, J., Shangguan, D., Wei, J., Bao, W., and Wu, L.: The contemporary glaciers in China based on the Second Chinese Glacier Inventory (in Chinese with English abstract), Acta Geographica Sinica, 70, 3, https://doi.org/10.11821/dlxb201501001, 2015.

Moorman, B. J., Robinson, S. D., and Burgess, M. M.: Imaging periglacial conditions with ground-penetrating radar, Permafrost and Periglacial Processes, 14, 319–329, https://doi.org/10.1002/ppp.463, 2003.

Mu, C., Zhang, T., Zhao, Q., Su, H., Wang, S., Cao, B., Peng, X., Wu, Q., and Wu, X.: Permafrost affects carbon exchange and its response to experimental warming on the northern Qinghai-Tibetan Plateau, Agricultural and Forest Meteorology, 247, 252 – 259, https://doi.org/https://doi.org/10.1016/j.agrformet.2017.08.009, 2017.

Nan, Z., Huang, P., and Zhao, L.: Permafrost distribution modeling and depth estimation in the Western Qinghai-Tibet Plateau (in Chinese with English abstract), Acta Geographica Sinica, 68, 318, https://doi.org/10.11821/xb201303003, 2013.

Norman, J., Kustas, W., and Humes, K.: Source approach for estimating soil and vegetation energy fluxes in observations of directional radiometric surface temperature, Agricultural and Forest Meteorology, 77, 263 – 293, thermal Remote Sensing of the Energy and Water Balance over Vegetation, 1995.

Prince, S., Goetz, S., Dubayah, R., Czajkowski, K., and Thawley, M.: Inference of surface and air temperature, atmospheric precipitable water and vapor pressure deficit using Advanced Very High-Resolution Radiometer satellite observations: comparison with field observations, Journal of Hydrology, 212-213, 230 – 249, https://doi.org/https://doi.org/10.1016/S0022-1694(98)00210-8, http://www.sciencedirect.com/science/article/pii/S0022169498002108, 1998.

Ran, Y., Li, X., Cheng, G., Zhang, T., Wu, Q., Jin, H., and Jin, R.: Distribution of Permafrost in China: An Overview of Existing Permafrost Maps, Permafrost and Periglacial Processes, 23, 322–333, https://doi.org/10.1002/ppp.1756, 2012.

Schmid, M.-O., Baral, P., Gruber, S., Shahi, S., Shrestha, T., Stumm, D., and Wester, P.: Assessment of permafrost distribution maps in the Hindu Kush Himalayan region using rock glaciers mapped in Google Earth, The Cryosphere, 9, 2089–2099, https://doi.org/10.5194/tc-9-2089-2015, https://www.the-cryosphere.net/9/2089/2015/, 2015.

Wang, W., Huang, X., Deng, J., Xie, H., and Liang, T.: Spatio-Temporal Change of Snow Cover and Its Response to Climate over the Tibetan Plateau Based on an Improved Daily Cloud-Free Snow Cover Product, Remote Sensing, 7, 169–194, https://doi.org/10.3390/rs70100169, 2015.

Wu, J., Sheng, Y., Wu, Q., and Wen, Z.: Processes and modes of permafrost degradation on the Qinghai-Tibet Plateau, Science in China Series D: Earth Sciences, 53, 150–158, https://doi.org/10.1007/s11430-009-0198-5, 2010.

Wu, Q. and Zhang, T.: Recent permafrost warming on the Qinghai-Tibetan Plateau, Journal of Geophysical Research: Atmospheres, 113, n/a–n/a, https://doi.org/10.1029/2007JD009539, d13108, 2008.

Wu, Q., Zhu, Y., and Liu, Y.: Application of the Permafrost Table Temperature and Thermal Offset Forecast Model in the Tibetan Plateau (in Chinese with English abstract), Journal of Glaciology and Geocryology, pp. 24–27, 2002.

Wu, Q., Zhang, Z., Gao, S., and Ma, W.: Thermal impacts of engineering activities and vegetation layer on permafrost in different alpine ecosystems of the Qinghai–Tibet Plateau, China, The Cryosphere, 10, 1695–1706, https://doi.org/10.5194/tc-10-1695-2016, 2016.

Wu, X., Nan, Z., Zhao, S., Zhao, L., and Cheng, G.: Spatial modeling of permafrost distribution and properties on the Qinghai–Tibet Plateau, Permafrost and Periglacial Processes, 29, 86–99, https://doi.org/10.1002/ppp.1971, 2018.

Yang, K., He, J., Tang, W., Qin, J., and Cheng, C. C.: On downward shortwave and longwave radiations over high altitude regions: Observation and modeling in the Tibetan Plateau, Agricultural and Forest Meteorology, 150, 38 – 46, https://doi.org/https://doi.org/10.1016/j.agrformet.2009.08.004, 2010.

Zhang, T.: Influence of the seasonal snow cover on the ground thermal regime: An overview, Reviews of Geophysics, 43, https://doi.org/10.1029/2004RG000157, 2005.

Zhang, T., Heginbottom, J. A., Barry, R. G., and Brown, J.: Further statistics on the distribution of permafrost and ground ice in the Northern Hemisphere, Polar Geography, 24, 126–131, https://doi.org/10.1080/10889370009377692, 2000.

Zhang, Y., Li, B., and Zheng, D.: A discussion on the boundary and area of the Tibetan Plateau in China, Geographical Research, 21, 1, https://doi.org/10.11821/yj2002010001, 2002.

Zhang, Y. L., Li, X., Cheng, G. D., Jin, H. J., Yang, D. W., Flerchinger, G. N., Chang, X. L., Wang, X., and Liang, J.: Influences of Topographic Shadows on the Thermal and Hydrological Processes in a Cold Region Mountainous Watershed in Northwest China, Journal of Advances in Modeling Earth Systems, 10, 1439–1457, https://doi.org/10.1029/2017MS001264, https://agupubs.onlinelibrary.wiley.com/doi/abs/10.1029/2017MS001264, 2018.

Zhao, S., Nan, Z., Huang, Y., and Zhao, L.: The Application and Evaluation of Simple Permafrost Distribution Models on the Qinghai—Tibet Plateau, Permafrost and Periglacial Processes, 28, 391–404, https://doi.org/10.1002/ppp.1939, 2017.

Zou, D., Zhao, L., Sheng, Y., Chen, J., Hu, G., Wu, T., Wu, J., Xie, C., Wu, X., Pang, Q., Wang, W., Du, E., Li, W., Liu, G., Li, J., Qin, Y., Qiao, Y., Wang, Z., Shi, J., and Cheng, G.: A new map of permafrost distribution on the Tibetan Plateau, The Cryosphere, 11, 2527–2542, https://doi.org/10.5194/tc-11-2527-2017, 2017.

Table 1. Classification algorithm of in-situ permafrost presence or absence evidence from various methods

Method	Indicator	Survey depth	Permafrost	Confidence degree
BH	MGT $\leqslant$ 0 °C	meters to about 20 m	presence	high
SP	ground ice presence	about 1.0–2.5 m	presence	high
GST	MAGST $\leqslant$ -2 °C & observations $\geqslant$ 3	0.05 or 0.1 m	presence	medium
	MAGST $\leqslant$ -2 °C & observations $<$ 3		presence	low
	MAGST $>$ -2 °C & $MAGST + TO_{\text{max}} \leqslant$ 0 °C		presence	low
	MAGST $<$ 0 °C & $MAGST + TO_{\text{max}} >$ 0 °C		ambiguous	–
	MAGST $>$ 0 °C		absence	medium
GPR	active layer thickness could be estimated	about 0.80–5.0 m	presence	medium

BH = borehole temperature, SP = soil pit, GST = ground surface temperature, GPR = ground-penetrating radar, MGT = mean ground temperature, and MAGST = mean annual ground surface temperature. TO_{max}, the maximum thermal offset under natural conditions reported for the QTP, is 0.79 °C. Ambiguous means the data is not sufficient to determine permafrost conditions and is not included in the inventory.

Table 2. Summary and evaluation of existing permafrost maps over the Qinghai-Tibet Plateau

Name	IPA	QTP_{TTOP}	QTP_{Noah}	PZI_{norm}	PZI_{warm}	PZI_{cold}
Year	1997	2017	2018	2012	2012	2012
Method	–	semi-physical model	physical model	heuristic GLM	heuristic GLM	heuristic GLM
Classification ~~Criteria~~ criteria	categorical	categorical	categorical	continuous	continuous	continuous
Scale	1:10,000,000	∼1 km	0.1° (∼10 km)	∼1 km	∼1 km	∼1 km
PCC_{PF} [%]	~~97.3~~ 46.6	93.9	96.4	76.6	35.3	94.3
PCC_{NPF} [%]	~~21.9~~ 79.8	58.6	45.9	82.6	98.5	54.0
PCC_{tol} [%]	~~73.8~~ 57.0	82.8	80.7	78.5	55.1	81.7
κ	~~0.32~~ 0.21	0.58	0.52	0.56	0.36	0.55
PF ~~Region~~ region [10^6 km^2]	1.63	–	–	1.68	1.42	1.84
PF ~~Area~~ area [10^6 km^2]	–	1.06 ± 0.09	1.13	1.00	0.76	1.25
Reference	Brown (1997)	Zou et al. (2017)	Wu et al. (2018)	Gruber (2012)	Gruber (2012)	Gruber (2012)

Evaluations are conducted using 1475 in-situ measurements of permafrost presence or absence. GLM = generalized linear model, PF = permafrost. Norm (normal), warm, and cold means different cases and assumptions of parameters for permafrost distribution simulations in the PZI_{global} map, details are from Table 1 of Gruber (2012). The continuous classification criteria means the permafrost spatial patterns is compiled or present as continuous value with a range of [0.01–1], e.g., permafrost zonation index in the PZI maps.

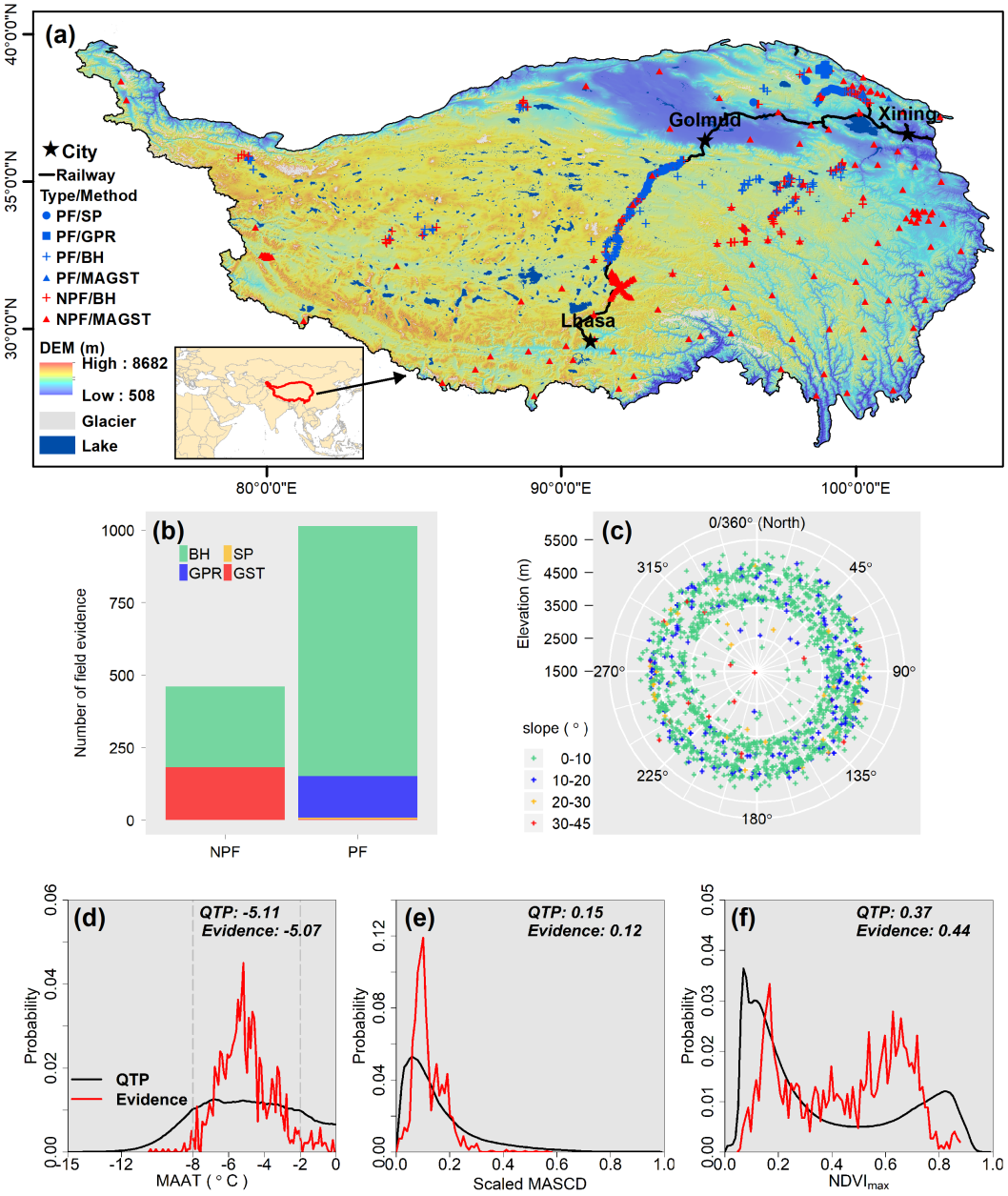

Figure 1. (a) The location of the QTP, and in-situ permafrost presence ~~/~~(PF) or absence (NPF) evidence distribution over the QTP, superimposed on the background of digital elevation model (DEM) with a spatial resolution of 30 ~~arcsec~~arc second. (~~e~~b) Number of field evidence located in ~~permafrost absence (~~NPF ~~)~~ and ~~presence (~~PF ~~)~~ regions. ~~BH~~ SP means soil pit, GPR refers ground-penetrating radar, BH stands field evidence measured by borehole drilling, ~~GPR means ground-penetrating radar, SP means soil pit,~~ and MAGST ~~means~~ is mean annual ground surface temperature. (~~d~~c) Distribution of field evidence in terms of elevation (radius), slope (colored), and aspect (0/360° represents North). ~~Spread~~ Distributions of ~~evidence (red line) for the climate variable of (~~d) mean annual air temperature (MAAT), (e) scaled mean annual snow cover days (MASCD), and (f) annual maximum NDVI ($NDVI_{max}$) for field evidence (red line) comparing to the entire QTP (black line). Numbers in (d), (e), and (f) are mean values. Only the sites ~~/plots~~ with MAAT < 0 °C, which is the precondition for permafrost presence, were present in (d).

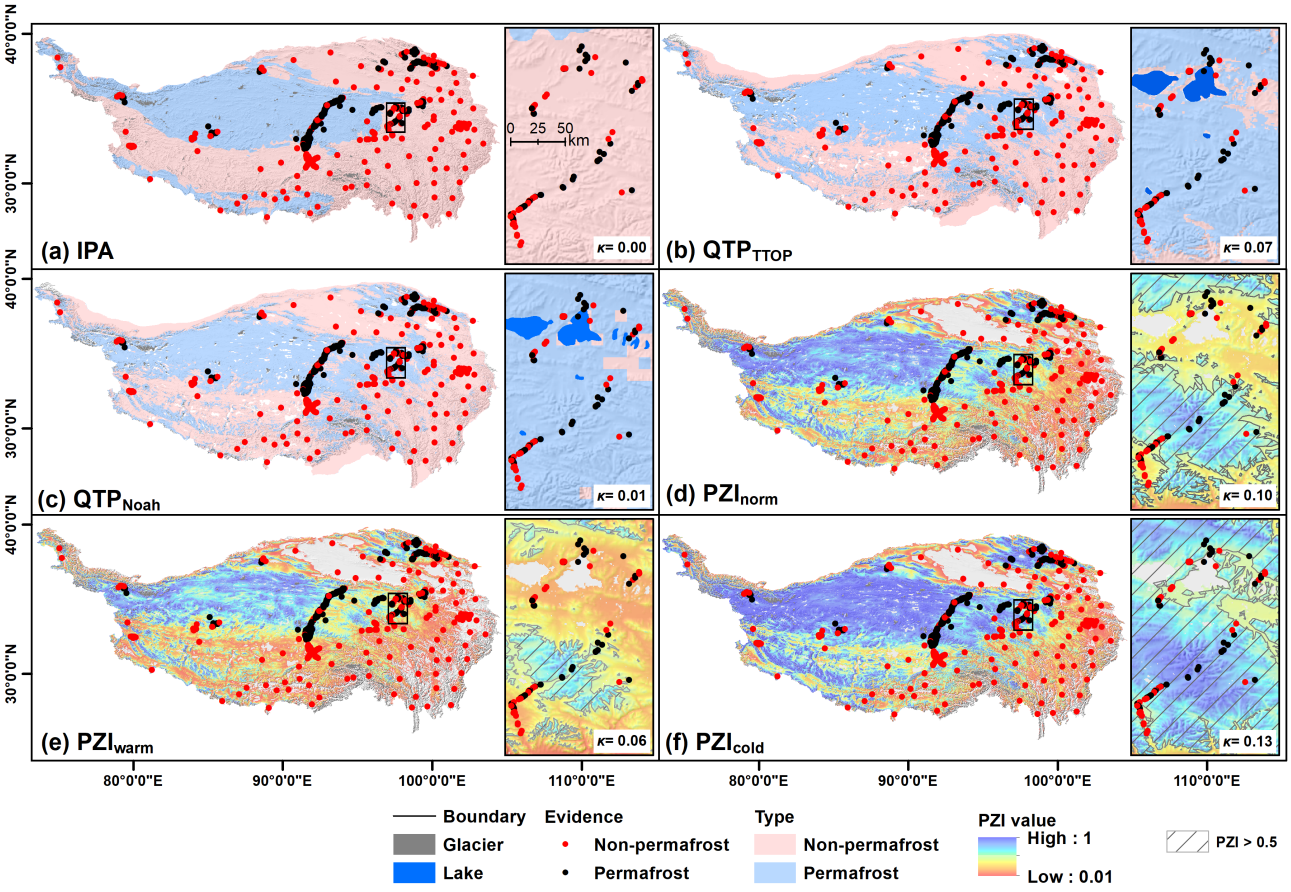

Figure 2. The permafrost classification results at in-situ evidence sites ~~/plots in~~ shown on the (a) IPA, (b) QTP$_{TTOP}$, (c) QTP$_{Noah}$, (d) PZI$_{norm}$, (e) PZI$_{warm}$, and (f) PZI$_{cold}$ maps. The Cohen's kappa coefficient (κ~~and PCC are~~), was derived from the ~~evaluation results for the~~ selected spatially highly variable landscapes (marked by black box) with 106 evidence sites. All the maps are re-sampled to the unprojected grid of SRTM30 DEM with a spatial resolution of 30 ~~arcsec~~ arc second (~1 km) to avoid maps bias ~~of with~~ caused by different resolutions, geographic projection, and format. The boundary of QTP used in this study is marked by black line. Categorical classification is used for ~~the~~ the QTP$_{TTOP}$, QTP$_{Noah}$, and IPA maps, while continuous PZI was present for the PZI$_{norm}$, PZI$_{warm}$, PZI$_{cold}$ maps. The blank ~~part~~ parts in the PZI maps ~~is area~~ are areas with PZI < 0.01.~~The κ and PCC_{tol} present in right small figures were evaluated in the selected areas with 106 evidence.~~

~~Classification algorithm of in-situ permafrost presence or absence evidence from various methods Method Indicator Survey depth Permafrost Confidence degreeBH MAGST $\leqslant$ 0 °Cmeters to about 20 m presence highSP ground ice presence about 1.0–2.5 m presence highGST MAGST $\leqslant$ -2 °C & observations $\geqslant$ 3 0.05 or 0.1 m presence mediumMAGST $\leqslant$ -2 °C & observations < 3 presence lowMAGST > -2 °C & $MAGST + TO_{max} \leqslant 0$ °Cpresence lowMAGST < 0 °C & $MAGST + TO_{max}$ > 0 °Cambiguous –MAGST > 0 °C absence mediumGPR clear permafrost reflection about 0.80–5.0 m presence medium~~